On the Nature of Instabilities of Traffic Flow – What Traffic Data and Mathematics can tell us

Martin Treiber[1] and Arne Kesting[1]

Technische Universität Dresden, Institute for Transport & Economics,
Würzburger Str. 35, 01187 Dresden, Germany

Abstract. We analyze detector data from several hundred traffic jams on freeways in Germany, Holland, England, and the USA with respect to the nature of traffic instabilities. By applying dedicated analyzing tools, we summarize the qualitative aspects in terms of the *stylized facts* of jam propagation. In the overwhelming majority of all cases, the data are compatible with linear string instabilities of the *convective* type, i.e., perturbations grow but eventually propagate out of the congested region. We quantify the instability in terms of linear growth rate, wavelength of the oscillations, and propagation velocity as a function of the empirically determined bottleneck strength. On the theoretical side, we derive analytical criteria for linear and convective stability applicable to a wide range of microscopic and macroscopic models and divide these models into five stability classes which uniquely determine the set of observable spatiotemporal patterns in real systems. Finally, we show, by means of approximate analytic solutions to systems with sustained localized noise (at the bottleneck) that controversial phenomena such as the "pinch effect" can be quantitatively explained by the phenomenon of convective instability using stability quantities that can be measured but also analytically derived from the corresponding microscopic or macroscopic model.

1 Introduction

In spite of investigating traffic flow dynamics for decades, some fundamental questions are not yet settled: Can the multitude of observed spatiotemporal patterns of congested traffic be decomposed into precisely defined elementary patterns? If so, into how many patterns, and what are their defining properties? Are there two or three traffic phases? Are typical instabilities of traffic flow of a nonlinear type requiring a finite perturbation for activation, or are they linear? Can insights into stability properties of closed ring roads be transferred to real open systems? Clearly, the last two questions are the most fundamental since instabilities are the main building block for dynamic traffic phases and spatiotemporal patterns.

In this contribution we show, by means of extensive empirical investigations and a quantitative analytical analysis, that the concept of *convective instability* may provide the missing link in understanding the traffic dynamics.

Section 2 presents qualitative aspects of the spatiotemporal evolution of congested traffic patterns (the *stylized facts*) as a result of analyzing traffic data from several freeways in Germany, Holland, England, and the USA. Section 3 quantifies the stylized facts of extended congestions by analyzing a large database

(containing more than 400 jams). The results are presented in form of scatter plots of the growth rate, wavelength, and propagation velocity of the oscillations as a function of the bottleneck strength. The main analytical results will be developed in the Sections 4 and 5. Section 4 gives compact criteria for local instability, convective string instability, and absolute string instability for a wide range of models and relates the patterns qualitatively to a newly formulated "class diagram". Finally, the observations of Sec. 3 are quantitatively and analytically related to solutions of car-following models in open systems with local sustained noise. The implications are discussed in Sec. 6.

2 Empirical Evidence

In this section, we will summarize the *stylized facts* of the spatiotemporal evolution of congested traffic patterns, i.e., qualitative empirical findings that are persistently observed on various freeways all over the world, e.g., the USA, Great Britain, the Netherlands, and Germany [1–4]. We will not list facts that are not directly related to the spatiotemporal evolution such as the wide scattering of flow-density data [5], or the movement of upstream jam fronts [6,2].

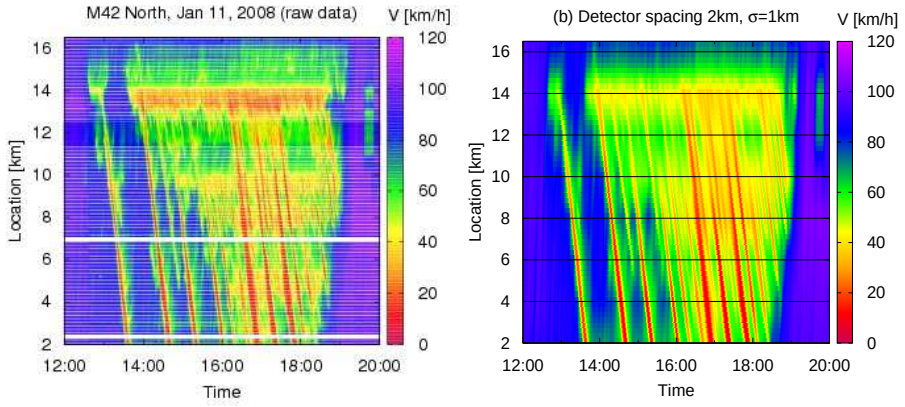

Fig. 1. Validation of the adaptive smoothing method. The ground truth (left) is compared with an ASM reconstruction assuming a detector spacing of 2 km (horizontal lines indicate detector locations).

A major difficulty for a systematic survey is the sparseness of the available data. With the exception of a few well-investigated freeway sections, the distance between detector cross sections does not allow to obtain spatiotemporal speed profiles by direct interpolation and smoothing. We therefore use a dedicated scheme, the adaptive smoothing method (ASM) [7,4] which makes use of some generally accepted properties of traffic flow to reconstruct the spatiotemporal profile from sparse data. To avoid circular reasoning (presenting facts that

alrady have been assumed), we have validated the ASM against extremely dense data (detectors every 100 m, sometimes 10 m) on the British motorway M42 near London, which can *de facto* be considered as ground truth. With detector information every two kilometers (cf. Fig. 1), the ASM could reconstruct the ground truth in great detail and turned out to be robust with respect to parameter changes [4]. This allows a systematic investigation resulting in the following list of stylized facts:

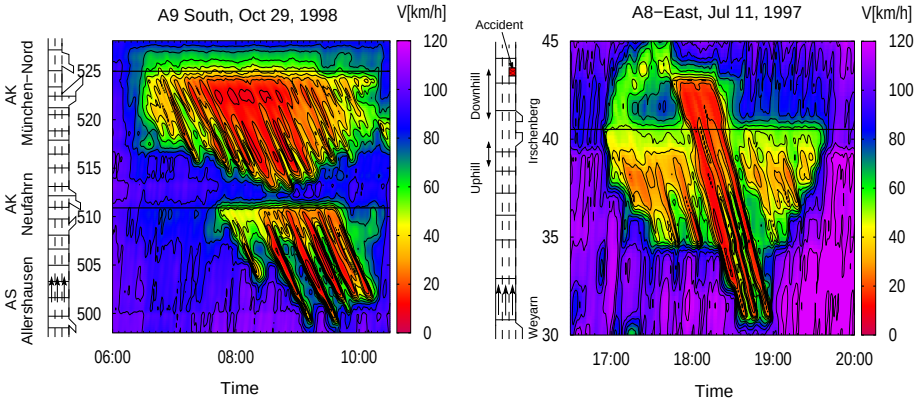

Fig. 2. Spatiotemporal dynamics of congestions on German freeways illustrating the stylized facts of congested traffic.

1. *Congestion patterns are typically caused by bottlenecks* in combination with a perturbation in the traffic flow. Analyzing about 400 congestion patterns on the German freeways A5-North and A5-South (Fig. 3) did not bring conclusive evidence of a single breakdown without a bottleneck [8]. The bottlenecks may be intersections (Fig. 2(a)), uphill or downhill gradients (the "Irschenberg" in Fig. 2(b) around $x = 40\,\mathrm{km}$), junctions (Fig. 2(b) at 41 km, or obstructions caused by accidents (Fig. 2(b) at $x = 43.5\,\mathrm{km}$ in the time period between 17:40 h and 18:15 h).
2. *The congestion pattern can be localized or spatially extended.* Localized congestion patterns either remain stationary at the bottleneck, or move upstream at a characteristic speed c_{cong} in form of isolated *stop-ang-go waves.* Typical values of c_{cong} are between $-20\,\mathrm{km/h}$ and $-15\,\mathrm{km/h}$, depending on the country and traffic composition [1], but not on the type of congestion.
3. *The downstream front is either fixed at the bottleneck or moves with the characteristic speed* c_{cong}. Both, fixed and moving downstream fronts can occur within one and the same congestion pattern when the bottleneck becomes weaker (Fig. 2(a) at $x = 510\,\mathrm{km}$) or ceases to exist (the accident in Fig. 2(b)).

4. *Most extended traffic patterns exhibit internal oscillations* propagating upstream approximately at the same characteristic speed c_{cong}. Consequently, all spatiotemporal structures of congested traffic in the figures of this paper (sometimes termed "oscillations", "stop-and-go traffic", or "small jams"), move in parallel [9,10,1].
5. *The frequency of the oscillations increases with the bottleneck strength.* For example, the strongest bottleneck in Fig. 2(a) is caused by the intersection "München Nord", and that in Fig. 2(b) by an accident.
6. *The amplitude of the oscillations increases while propagating upstream.* This can be seen in *all* empirical data shown in this contribution, see also Refs. [11,2,12]. Consequently, the downstream boundary is often stationary or shows little oscillations. At the upstream end of the congested area, the oscillations may eventually become isolated "wide jams" (Fig. 1 before 16:00 h; some of the congestions of Fig. 3), or remain part of a compact congestion pattern (Fig. 2, and again Fig. 3).
7. *Light or very strong bottlenecks may cause homogeneous congestions* (Figs. 1(d) and 1(f) of Ref. [2]).

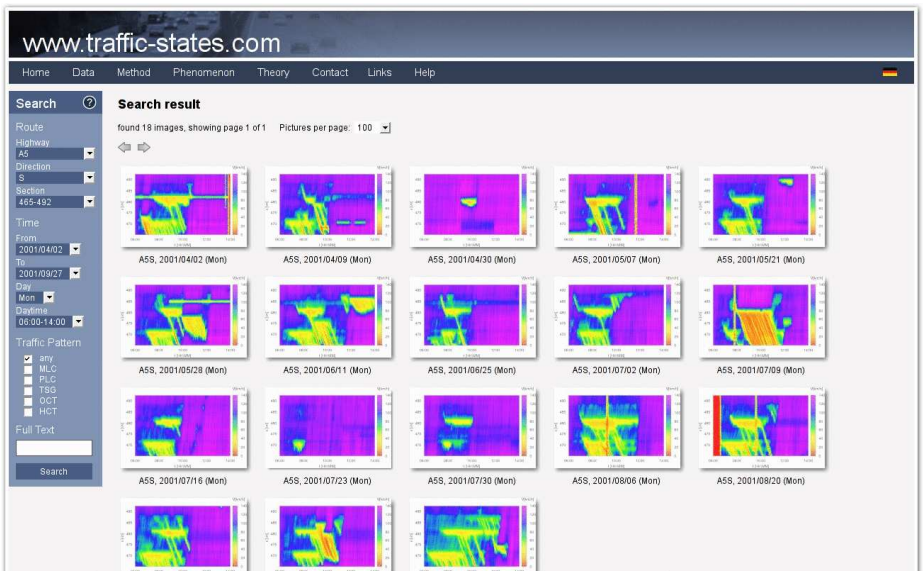

Fig. 3. Screenshot of a publicly available image database of congestions on the German freeway A5. The database can be searched by criteria such as direction of travel, space interval, time interval, weekday, cause of the congestion, or the type of traffic pattern.

3 Quantifying the Propagation of Traffic Waves

One of the most controversial phenomena is an observed spatiotemporal structure called the *"pinch effect"* or *"general pattern"* [13]. In the light of the *stylized facts* this spatiotemporal pattern follows from the Fact 6 (the oscillations grow while propagating upstream) in combination with Facts 1, 3, and 4. To get further insights, we have quantified the relevant *stylized facts* by a systematic analysis of about 400 congested traffic patterns on the German Autobahn A5 [14] (see Fig. 3) focussing on the about 200 extended congestion patterns of this database.

Figure 4 shows a set of measured speed time series for a typical extended jam: While the detectors close to the bottleneck (at $x = 482\,\mathrm{km}$ in Fig. 4(a)) show little oscillations (Facts 1 and 3), the oscillations grow in amplitude with the distance to the bottleneck in the upstream direction (Fact 6). Furthermore, the oscillations show a typical period (Fact 5), and they propagate with a certain velocity (Fact 4). We have quantified each of these aspects as follows:

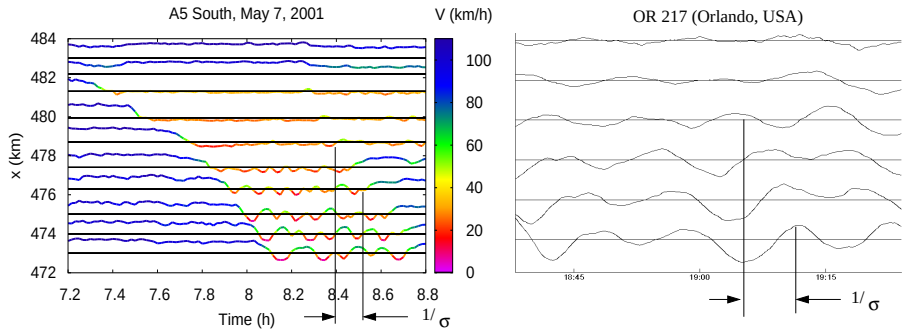

Fig. 4. Speed time series of several detectors on the German A9 and an American freeway [1]. Shown are deviations (oscillating curves) from the average speed (horizontal baselines). The detector spacings are proportional to the spacings of the baselines.

- The propagation velocity c_{cong} has been calculated by maximizing the sum of cross correlation functions of speed time series of detector pairs $\{i, j\}$ in the congested region (at positions x_i and x_j, respectively), with respect to the velocity c [1]:

$$c_{\mathrm{cong}} = \arg\max_{c} \sum_{i} \sum_{j>i} \mathrm{Corr}\left[V_i(t), V_j\left(t + \frac{x_i - x_j}{c}\right)\right]. \qquad (1)$$

  Notice that the time interval for calculating the correlation functions must be restricted such that the time series are only evaluated during congested or stop-and-go traffic.

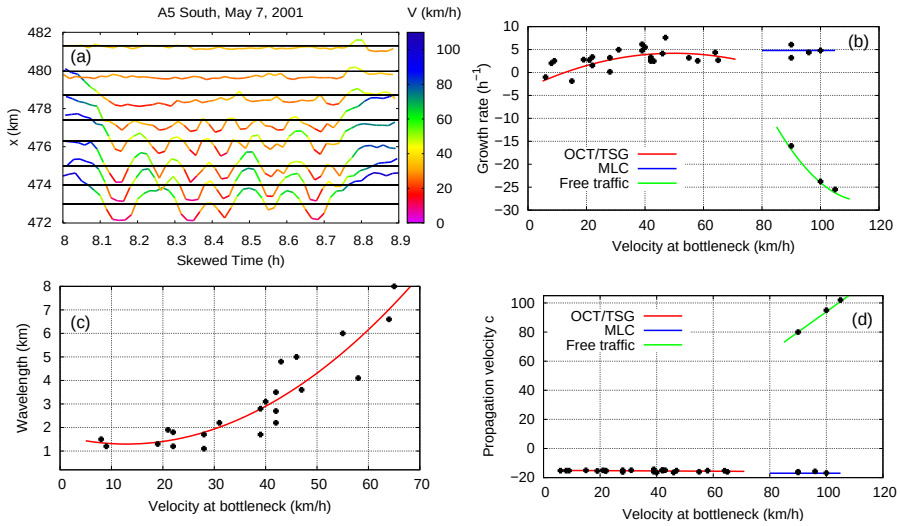

Fig. 5. Characteristic properties of the propagation of perturbations in congested traffic. (a) Speed time series with a skewed time axis; (b)-(d) quantities of jam propagation as a function of the speed near the bottleneck characterizing the bottleneck strength.

- The average period τ of the oscillations is given by the position of the first nontrivial peak of the autocorrelation functions of detector time series, again restricted to periods of congested traffic.
- The wavelength is given by $L_{\text{wave}} = \tau |c_{\text{cong}}|$.
- The average spatial growth rate $\tilde{\sigma}$ of perturbations is defined in terms of the slope of the linear regression of the data points $\{(x_i, \ln|A_i|\}$ consisting of the location x_i of the detectors and the logarithm of the amplitudes $|A_i|$ of the oscillations:

$$\tilde{\sigma} = \frac{\sum_i x_i \ln|A_i| - n\bar{x}\,\overline{\ln|A_i|}}{\sum_i x_i^2 - n\bar{x}^2}. \tag{2}$$

- The corresponding temporal growthrate is given by

$$\sigma = c_{\text{cong}}\tilde{\sigma}. \tag{3}$$

For example, the detector data shown in the Figs 4(a) or 5(a) result in $c_{\text{cong}} \approx -16\,\text{km/h}$, $\tau \approx 6\,\text{min}$ (for small amplitudes; some waves merge while growing), $L_{\text{wave}} \approx 1.6\,\text{km}$ (for small amplitudes), $\tilde{\sigma} \approx -0.4\,\text{km}^{-1}$, and $\sigma \approx 6.4\,\text{h}^{-1}$.

Using the above definitions, we have calculated the quantities c_{cong}, σ, and L_{wave} for the extended jams on the A5-South. In the Figures 5(b)-(d), they are plotted as a function of the average speed V_{cong} of the detector nearest to the downstream front, i.e., to the bottleneck. The speed V_{cong} serves as an observable proxy for the bottleneck strength: The lower V_{cong}, the stronger the bottleneck. Notice that, according to the Facts 3 and 6, the traffic flow at this location is essentially stationary, so this speed is well defined.

The analysis quantitatively confirms the stylized facts presented in Sec. 2. Moreover, the local growth rates $\tilde{\sigma}_i = (\ln|A_i| - \ln|A_{i-1}|)/(x_i - x_{i-1})$ resulting from Eq. (2) for a pair of neighboring detectors do not depend significantly on the amplitude, at least, if the oscillations can be distinguished from noise, and if nonlinear saturation has not yet set in. This means, there is no empirical evidence against the existence of linear instabilities in congested traffic.

4 Stability Analysis

There are several stability types pertaining to traffic flow (cf. Fig. 6). *Local instability* implies that sustained oscillations already arise when a single vehicle follows a leader driving at a constant speed. Much more restrictive and relevant is the *string instability* of a platoon of vehicles following each other. Here, a positive feedback between gaps and velocities of adjacent vehicles leads to growing oscillations even if each driver is perfectly able to follow a single leader with damped or even without oscillations [15]. Morover, there are two subtypes: If the string instability is *convective*, the growing oscillations propagate in only one direction (against the driving direction). Consequently, in realistic open systems, they eventually leave the road section. In contrast, when the string instability is *absolute*, perturbations propagate in both directions eventually leading to sustained oscillations everywhere. Notice that this distinction does not exist in closed systems (ring roads).

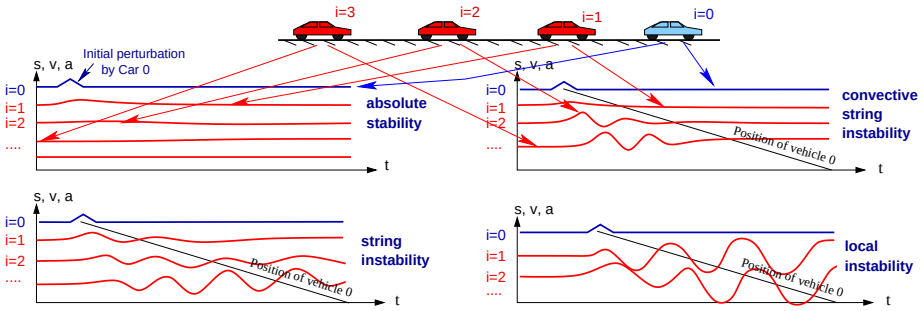

Fig. 6. Visualization of the different stability concepts relevant for traffic flow in form of time series (left column) and spatiotemporal dynamics (right column).

Furthermore, the instabilities discussed above may be linear (can be triggered by an infinitesimal perturbation), or nonlinear (a finite perturbation is necessary). In the latter case, one also speaks of *metastability*. Remarkably, in describing the observed congestion patterns, the distinction between the absolute and convective nature of instabilities will prove to be more important than the distinction between linear and nonlinear instabilities.

We now give the condition for string instability for general car-following models[1] with equation of the form

$$\frac{\mathrm{d}x_\alpha}{\mathrm{d}t} = v_\alpha, \tag{4}$$

$$\frac{\mathrm{d}v_\alpha}{\mathrm{d}t} = a_{\mathrm{mic}}\left(s_\alpha(t), v_\alpha(t), v_{\alpha-1}(t)\right). \tag{5}$$

Here, vehicle $\alpha-1$ precedes vehicle α, and the spatial gap $s_\alpha = x_{\alpha-1} - x_\alpha - l_{\alpha-1}$ is given by the vehicle distance minus the length of the leading vehicle. The microscopic acceleration function $a_{\mathrm{mic}}(s, v, v_l)$ characterizes the specific model and describes the acceleration as a function of the gap, the own speed and the speed v_l of the leader. The homogeneous-stationary equilibrium state of such models is given by the condition $a_{\mathrm{mic}}\big(s, v_e(s), v_e(s)\big) = 0$ defining the equilibrium speed $v_\alpha(t) = v_e$ as a function of the gap s (microscopic fundamental diagram). This state is string instable if

$$v_e'(s_e) > \frac{1}{2}\left(\left.\frac{\partial a_{\mathrm{mic}}}{\partial v_l}\right|_e - \left.\frac{\partial a_{\mathrm{mic}}}{\partial v}\right|_e \right), \tag{6}$$

where the subscript e stands for "taken at equilibrium". A typical example of such a model is the Intelligent Driver Model (IDM) [16] which is characterized by the acceleration function.

$$a_{\mathrm{IDM}}(s, v, v_l) = a\left[1 - \left(\frac{v}{v_0}\right)^4 - \left(\frac{s^*}{s}\right)^2\right], \quad s^* = s_0 + vT + \frac{v(v-v_l)}{2\sqrt{ab}}, \tag{7}$$

where v_0 is the desired speed, a and b are comfortable accelerations and decelerations, s_0 denotes the minimum gap, and T the desired time headway in car-following situations. For this model, the instability criterion (6) becomes

$$(v_e')^2 > \frac{a(s_0 + v_e T)}{s_e^2}\left[\frac{s_0 + v_e T}{s_e} + \frac{v_e v_e'}{\sqrt{ab}}\right]. \tag{8}$$

For the limiting case of very congested traffic, $s_e \to s_0$, this simplifies to $a < s_0/T^2$.

If homogeneous traffic flow is linearly string instable, there exists a range of wave numbers k where the associated wave solutions $\propto e^{\lambda(k)t + i\alpha k}$ of the linearized equations (where λ is the analytically given complex growth rate and i is the imaginary unit) display a positive growth rate $\sigma(k) = \mathrm{Re}(\lambda(k))$. In particular, there is a certain finite wave number $k_0 = \arg\max_k \sigma(k)$ associated with the maximum growth rate $\sigma_0 = \sigma(k_0) > 0$. It can be shown that an approximate criterion for convective instability is given by

$$0 < \sigma_0 \le \frac{v_g^2}{2D_2}, \tag{9}$$

[1] A similar stability criterion can be given for general (local or nonlocal) macroscopic models formulated in terms of PDEs.

where the group velocity v_g and the dispersion coefficient D are given in terms of derivatives of the complex growth rate $\lambda(k) = \sigma(k) + i\omega(k)$:

$$v_g = v_e + \frac{\omega'(k_0)}{\rho_e}, \quad D_2 = -\frac{\sigma''(k_0)}{\rho_e^2}\left[1 + \left(\frac{\omega''(k_0)}{\sigma''(k_0)}\right)^2\right], \quad \rho_e = \frac{1}{l + s_e}. \tag{10}$$

It should be noted that this criterion implies that the linear string instability *always* starts as a convective one. Often, the instability remains convective for the whole range of equilibrium densities (Fig. 7(a),(b)). For typical congested situations, v_g is of the order of (but not equal to) the propagation velocity c_{cong}, and D is of the order of $500\,\text{m}^2/\text{s}$. Simulations with the IDM show that criterion (9) defines the actual density range of convective instability, e.g. that of Fig. 7(d), with errors below 1%.

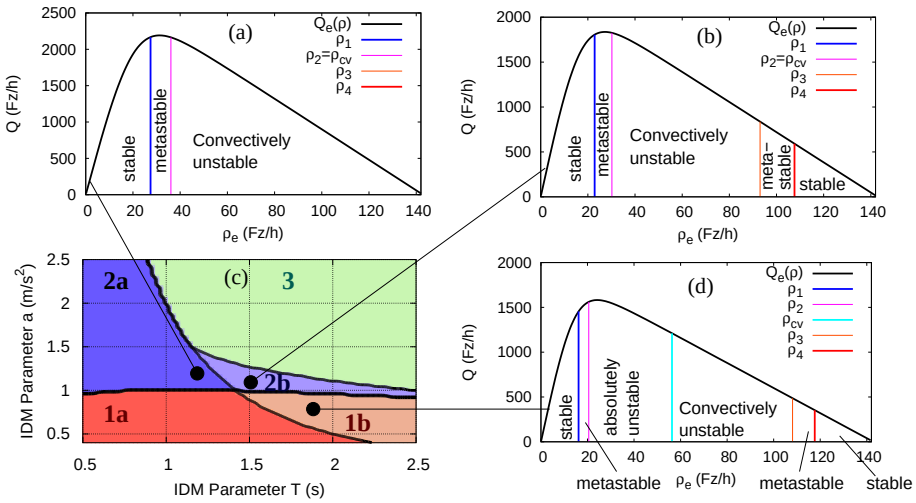

Fig. 7. Class diagram of the IDM for $v_0 = 120\,\text{km/h}$, $s_0 = 2\,\text{m}$, and $b = 1.5\,\text{m/s}^2$ as a function of the time gap T and acceleration a, and stability diagrams for three points of the class diagram corresponding to the class 1b, 2a, and 2b.

The overall stability properties of a traffic flow model are given by the *stability diagram* denoting the stability type for all possible equilibrium states parametrized by the associated density $\rho = 1/(s_e + l)$ (see Fig. 7(a),(b),(d)). Generally, one obtains several density regions with the boundaries $0 < \rho_1 < \rho_2 \leq \rho_{cv} < \rho_3 \leq \rho_4 \leq \rho_{\max}$. Homogeneous traffic flow is absolutely stable for $\rho < \rho_1$ or $\rho \geq \rho_4$, metastable for $\rho \in [\rho_1, \rho_2]$ or $[\rho_3, \rho_4]$, convectively unstable for $\rho \in [\rho_2, \rho_{cv}]$, and absolutely unstable for $\rho \in [\rho_{cv}, \rho_3]$. Furthermore, the number and types of traffic patterns do not only depend on the set of observed stability types, but also on the relative position of the stability boundaries with respect

to the density at (static) capacity $\rho_K = \arg\max_\rho Q_e(\rho)$. This leads to following stability classes (cf. Fig. 7):

- *Class 1a:* Traffic at capacity is (linearly) unstable, $\rho_2 < \rho_K$, and remains so for all higher densities, $\rho_3 = \rho_4 = \rho_{\max}$. Furthermore, $\rho_K < \rho_{cv} < \rho_{\max}$, i.e., the instability is absolute for comparatively light congested traffic and becomes convective for higher densities.
- *Class 1b:* As class 1a, but traffic restabilizes for heavily congested traffic, $\rho_3 < \rho_{\max}$.
- *Class 2a:* Traffic at capacity is metastable or stable, and unstable for sufficiently high densities, $\rho_K < \rho_2 < \rho_3 = \rho_{\max}$, In most cases, the instability is purely convective, but a small region of absolute instability is possible as well.
- *Class2b:* As class 2a, but with restabilization, $\rho_3 < \rho_{\max}$.
- *Class 3:* Unconditionally stable.

The stability class depends on the model and on the parameters. Some models can even be "tuned" to any stability class. Figure 7 displays such a "class diagram" for the IDM.

The stability and class diagrams are crucial for a possible explanation of the observed extended traffic patterns. The reasoning is as follows: After a traffic breakdown at a bottleneck, the average traffic flow of the congested state upstream is determined by the *dynamic capacity* $K_{\text{dyn}} = K(1-\epsilon)$ of the bottleneck (which is smaller than the static capacity by a capacity drop of the order of $\epsilon = 10\%$). Consequently, the congestion pattern depends on the stability properties of congested traffic at flow K_{dyn}:

For **stability class 1**, small bottlenecks (high values of K_{dyn}) correspond to absolutely unstable traffic, i.e., congested traffic is non-stationary everywhere and consists of a sequence of stop-and-go waves triggered by the bottleneck (TSG) [2]. The smaller the bottleneck, the lower the difference $Q_{\text{out}} - K_{\text{dyn}}$ between the outflow of the waves and the bottleneck capacity, i.e., the longer it takes until there is a sufficient number of vehicles to trigger the next stop-and-go wave. Conversely, the wave frequency increases with the bottleneck strength until the stop-and go waves are no longer isolated but part of oscillatory congested traffic (OCT). For class 1b, traffic becomes stable for very strong bottlenecks resulting in homogeneous congested traffic (HCT). For class 1b, OCT (with very high frequencies) persists until the complete standstill.

For **stability class 2**, congested traffic is linearly stable for very small bottlenecks, so a new high-flow homogeneous states (homogeneous synchronized traffic, HST) is possible [2]. However, since traffic generally is metastable in this situation, stronger perturbations can lead to stop-and-go waves as well. When increasing the bottleneck strength, one obtains OCT (class 2a) or the sequence OCT-HCT (class 2b), similarly to stability class 1. Unlike class 1, however, the instability is nearly always a convective one, so perturbations grow, but only in upstream direction. As will be shown analytically in the next section, this leads to essentially stationary traffic flow near the bottleneck *even if sustained finite perturbations are present.*

For **stability class 3**, congested traffic is always essentially homogeneous, and the dynamics similar to that of first-order (Lighthill-Witham-Richards) models [6].

5 Sustained Perturbations

Finally we will show, by means of approximate but quantitative analytical calculations, how convectively unstable flow in combination with sustained perturbations (caused, e.g., by mergings at onramps or offramps) will lead to stationary flow near the source of the perturbations, and growing oscillations further upstream. To this end, we investigate the statistical properties of the model (5) with an additional localized noise term,

$$\frac{\mathrm{d}v_\alpha}{\mathrm{d}t} = a_{\mathrm{mic}}\left(s_\alpha(t), v_\alpha(t), v_{\alpha-1}(t)\right) + \frac{\xi_\alpha}{v_\alpha}\delta(x_\alpha(t)). \tag{11}$$

Here, $\delta(x)$ is the δ-distribution, i.e., $\int \mathrm{d}x f(x)\delta(x) = f(0)$ for any localized function f, and ξ_α are realizations of independent standard-normally distributed stochastic variables. Thus, whenever a car crosses $x = 0$, its speed is abruptly changed by ξ_α.

Since we are interested in the collective properties of oscillations, it is sufficient to investigate the statistical properties of an approximate macroscopic speed field $V_1(x,t)$ representing the local deviations from the equilibrium speed v_e. In the linear regime, the realizations of this velocity field are given by

$$V_1(x,t) \propto \int_0^\infty \mathrm{d}\tau\, G(x,\tau)\xi(t-\tau), \quad \langle\xi(t)\rangle = 0, \quad \langle\xi(t)\xi(t')\rangle = \delta(t-t'). \tag{12}$$

The "Green's function" $G(x,t)$ is defined by the linear spatiotemporal response of equilibrium flow to a single localized perturbation of unit strength at $x = 0$, $t = 0$. A long calculation shows that approximatively $G(x,t) = \mathrm{Re}\,\tilde{G}(x,t)$, where

$$\tilde{G}(x,t) = \exp(ik_0x - i\omega_0t)\, A(x,t), \quad A(x,t) = \exp\left[\left(\sigma_0 - \frac{\left(v_g - \frac{x}{t}\right)^2}{2\lambda_2}\right)t\right], \tag{13}$$

with $\lambda_2 = -\sigma''(k_0) + i\omega''(k_0)$. Figure 8(a) shows the Green's function for traffic flow at the limit between convective and absolute instability. To assess the validity of the various approximations leading to Eq. (13), the analytical result is compared with the simulation of the same system (cf. Fig. 8(b)) resulting in a nearly perfect agreement.

The stochastic properties of the solution (12) (a realization is shown in Fig. 9 (a)) can be described by the structure function

$$S(x,x',t,t') = \langle V_1(x,t)V_1(x',t')\rangle. \tag{14}$$

Inserting Eqs. (12) and (13) and dropping some prefactors leads to an approx-

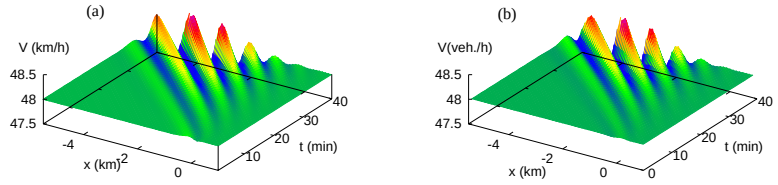

Fig. 8. Traffic flow at the limit between convective and absolute string instability (IDM, $a = 1.05\,\mathrm{m/s^2}$, $T = 1.5\,\mathrm{s}$; other parameters as in Fig. 7). Shown is the response to a single perturbation in form of the macroscopic speed field (a) according to the analytical expression (13), (b) for the IDM simulation.

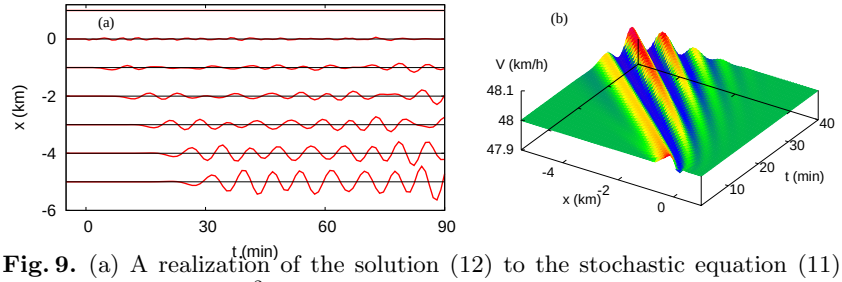

Fig. 9. (a) A realization of the solution (12) to the stochastic equation (11) for the IDM with $a = 1.11\,\mathrm{m/s^2}$ and the other parameters as in Fig. 8; (b) the corresponding Green's function.

imate analytic expression for the speed variance:

$$S(x,x,t,t) \sim \frac{1}{\sqrt{1-\frac{2D_2\sigma_0}{v_g^2}}} \exp\left[\frac{2xv_g}{D_2}\left(1-\sqrt{1-\frac{2D_2\sigma_0}{v_g^2}}\right)\right]. \qquad (15)$$

This expression is valid if $v_g x/(2D_2)\sqrt{1-2\sigma_0 D_2/v_g^2} \gg 1$, i.e., sufficiently far away from the threshold to abolute instability and from the source of the perturbations. (The left-hand side is equal to $x/850\,\mathrm{m}$ for the parameters of Fig. 9).

We observe that, in spite of linear instability and sustained noise, the variance remains finite in the convectively unstable regime. Furthermore, the variance depends only on x, i.e., the solution is stationary in the stochastic sense. The oscillations grow in the upstream direction (notice that $v_g < 0$). From Eq. (15), one can extract a quantity that is observable from the realizations $V_1(x,t)$, Fig. 9(a), or from traffic data, Fig. 5(a): The distance L in which the amplitude grows by a factor of e is given by

$$L = \frac{D_2}{v_g}\left(1-\sqrt{1-\frac{2D_2\sigma_0}{v_g^2}}\right)^{-1}. \qquad (16)$$

For the IDM parameters of Fig. 9, one obtains a physical wavelength $2\pi k_0/\rho_e = 1.5\,\mathrm{km}$, a maximum growth rate $\sigma_0 = 3.0\,\mathrm{h^{-1}}$, and $L = 2.5\,\mathrm{km}$. This is consistent

with the spatial growth rate $\tilde{\sigma} = 1/L = 0.4\,\mathrm{km}^{-1}$ as determined from Fig. 5(a). Notice that the growth rate $\tilde{\sigma} v_\phi = 4.4\,\mathrm{h}^{-1}$ *inferred* from detector time series by multiplying the spatial growth rate with the observable phase velocity (see Fig. 5(a)) is higher than the *maximum* linear growth rate σ_0.

6 Conclusion

In order to gain qualitative and quantitative insight into the nature of instabilities of traffic flow, we have analyzed a large database of congested traffic and other traffic data around the world. Besides summarizing the qualitative aspects in form of a list of "stylized facts", we give quantitative detail of the key factors of congested traffic instabilities (wavelength, growth rate and propagation velocity as a function of the bottleneck strength) by a systematic analysis of about 400 congested patterns. Notably, we found positive perturbation growth rates for most instances of congestions and no empirical evidence against the existence of linear instabilities.

To understand the observations, one must relate them to mathematical models and theoretical concepts, preferably analytically and quantitatively ones. To this end, we define all relevant theoretical stability concepts and give analytic criteria for local instability, convective string instability, and absolute string instability of car-following models formulated in continuous time. Although some approximations have been used in deriving the analytical threshold between convective and absolute instability, it has been verified by simulations within observation uncertainty (about 1 % of the width of the convectively unstable region). Ongoing investigations show that the same analysis is possible for local and nonlocal macroscopic models formulated as partial differential equations.

We found new insight into the nature of traffic flow instabilities on two levels. On the qualitative level, we could relate the observed *stylized facts*, i.e., spatiotemporal patterns, to three "stability classes" (and two subclasses) derived from the stability diagram, i.e., from the set of density regions where a certain stability type applies. The original "phase diagram" of Ref. [17] was derived for stability class 1b, but other classes can lead to different sets of patetrns, and also to new patterns. The stability class depends not only on the model but also on the parameters. Moreover, the Intelligent Driver Model (IDM) can assume any stability class which leads to a "class diagram" in parameter space.

On the quantitative level, we have analytically related the observables of the "pinch effect" (oscillations of detector time series) with convectively unstable flow in an open system with sustained local noise (caused, e.g., by mandatory lane changes at lane closings, onramps, or offramps). The analytic solution (which, again, is verified by simulations) corresponds to stationary traffic flow near the bottleneck *even for linearly unstable traffic in the presence of sustained perturbations*, and to growing oscillations further upstream. When evaluated for the IDM, the associated wavelengths, growth rates and propagation velocities are in agreement with that derived from the data.

In conclusion, there is much evidence that the largely neglected concept of *convective instability* provides the final missing link in explaining the dynamics of congested traffic flow.

References

1. B. Zielke, R. Bertini, and M. Treiber, "Empirical Measurement of Freeway Oscillation Characteristics: An International Comparison," Transportation Research Record **2088,** 57–67 (2008).
2. D. Helbing, M. Treiber, A. Kesting, and M. Schönhof, "Theoretical vs. Empirical Classification and Prediction of Congested Traffic States," The European Physical Journal B **69,** 583–598 (2009).
3. R. Wilson, "Mechanisms for spatio-temporal pattern formation in highway traffic models," Philosophical Transactions of the Royal Society A **366,** 2017–2032 (2008).
4. M. Treiber, A. Kesting, and R. E. Wilson, "Reconstructing the Traffic State by Fusion of Heterogenous Data," accepted for publication in Computer-Aided Civil and Infrastructure Engineering, preprint `physics/0900.4467` (2009).
5. M. Treiber, A. Kesting, and D. Helbing, "Understanding widely scattered traffic flows, the capacity drop, and platoons as effects of variance-driven time gaps," Physical Review E **74,** 016123 (2006).
6. M. Lighthill and G. Whitham, "On kinematic waves: II. A theory of traffic on long crowded roads," Proc. Roy. Soc. of London A **229,** 317–345 (1955).
7. M. Treiber and D. Helbing, "Reconstructing the Spatio-Temporal Traffic Dynamics from Stationary Detector Data," Cooper@tive Tr@nsport@tion Dyn@mics **1,** 3.1–3.24 (2002), (Internet Journal, `www.TrafficForum.org/journal`).
8. M. Schönhof and D. Helbing, "Empirical features of congested traffic states and their implications for traffic modeling," Transportation Science **41,** 1–32 (2007).
9. C. F. Daganzo, "A behavioral theory of multi-lane traffic flow. Part I: Long homogeneous freeway sections," Transportation Research Part B: Methodological **36,** 131–158 (2002).
10. M. Mauch and M. J. Cassidy, "Freeway traffic oscillations: observations and predictions," in *International Symposium of Traffic and Transportation Theory*, M. Taylor, ed., (Elsevier, Amsterdam, 2002).
11. M. Schönhof and D. Helbing, "Critisism of three-phase traffic theory," Transporation Research Part B: Methodological **43,** 784–797 (2009).
12. M. Treiber, A. Kesting, and D. Helbing, "Three-phase traffic theory and two-phase models with a fundamental diagram in the light of empirical stylized facts," Transportation Research Part B: Methodology (submitted) (2009).
13. B. Kerner and H. Rehborn, "Experimental properties of complexity in traffic flow," Physical Review E **53,** R4275–R4278 (1996).
14. A. Kesting and M. Treiber, "`http://www.traffic-states.com`,", 2010.
15. A. Kesting and M. Treiber, "How reaction time, update time and adaptation time influence the stability of traffic flow," Computer-Aided Civil and Infrastructure Engineering **23,** 125–137 (2008).
16. M. Treiber, A. Hennecke, and D. Helbing, "Congested traffic states in empirical observations and microscopic simulations," Physical Review E **62,** 1805–1824 (2000).
17. D. Helbing, A. Hennecke, and M. Treiber, "Phase diagram of traffic states in the presence of inhomogeneities," Physical Review Letters **82,** 4360–4363 (1999).